UCRL-18229

cy. 2

University of California

Ernest O. Lawrence Radiation Laboratory

FAR-INFRARED SPECTRA OF Al_2O_3 DOPED WITH Ti, V, AND Cr

R. R. Joyce and P. L. Richards

June 1968

TWO-WEEK LOAN COPY

This is a Library Circulating Copy which may be borrowed for two weeks. For a personal retention copy, call Tech. Info. Division, Ext. 5545

REC
LA
RADIATIO
JUL 24 1968
LIBRARY AND
DOCUMENTS SECTION

Berkeley, California

UCRL-18229
Cy. 2

DISCLAIMER

This document was prepared as an account of work sponsored by the United States Government. While this document is believed to contain correct information, neither the United States Government nor any agency thereof, nor the Regents of the University of California, nor any of their employees, makes any warranty, express or implied, or assumes any legal responsibility for the accuracy, completeness, or usefulness of any information, apparatus, product, or process disclosed, or represents that its use would not infringe privately owned rights. Reference herein to any specific commercial product, process, or service by its trade name, trademark, manufacturer, or otherwise, does not necessarily constitute or imply its endorsement, recommendation, or favoring by the United States Government or any agency thereof, or the Regents of the University of California. The views and opinions of authors expressed herein do not necessarily state or reflect those of the United States Government or any agency thereof or the Regents of the University of California.

UCRL-18229
UC-4 Chemistry
TID-4500 (52nd Ed.)

UNIVERSITY OF CALIFORNIA

Lawrence Radiation Laboratory
Berkeley, California

AEC Contract No. W-7405-eng-48

FAR-INFRARED SPECTRA OF Al_2O_3 DOPED WITH Ti, V, AND Cr

R. R. Joyce and P. L. Richards

June 1968

Printed in the United States of America
Available from
Clearinghouse for Federal Scientific and Technical Information
National Bureau of Standards, U. S. Department of Commerce
Springfield, Virginia 22151
Price: Printed Copy $3.00; Microfiche $0.65

FAR-INFRARED SPECTRA OF Al_2O_3 DOPED WITH Ti, V, AND Cr

R. R. Joyce and P. L. Richards

Inorganic Materials Research Division, Lawrence Radiation Laboratory,
Department of Physics, University of California,
Berkeley, California

ABSTRACT

The absorption spectrum of samples of Al_2O_3 doped with Ti, V, and Cr has been measured at 4.2°K over the frequency range 5-120 cm^{-1}, in applied magnetic fields up to 55 kOe. In Al_2O_3:Ti absorption lines were observed at 37.8 cm^{-1} and 107 cm^{-1}; these were due to transitions between the ground and first excited states of the Ti^{3+} ion in a modified Al_2O_3 crystalline field. The Zeeman splitting of the observed lines yielded $g_{0\parallel} = 1.11 \pm .03$, $g_{1\parallel} = 2.00 \pm .06$, and $g_{0\perp}$, $g_{1\perp} < 0.1$ for the ground and first excited states. Similar results were observed from the isoelectronic V^{4+} ion in the Al_2O_3:V sample. Zero field absorption lines were observed at 28.1 cm^{-1} and 53 cm^{-1}, with g-values for the ground and first excited states of $g_{0\parallel} = g_{1\parallel} = 1.43 \pm .04$ and $g_{0\perp}$, $g_{1\perp} < 0.2$. The predicted energy levels of a single d electron in the Al_2O_3 crystalline field modified by a dynamic Jahn-Teller effect fit these data quite well. An absorption line observed at 8.25 cm^{-1} in Al_2O_3:V was attributed to the spin-orbit splitting of the lowest electronic state of the V^{3+} ion. The Zeeman splitting of this line is in excellent agreement with the appropriate spin-Hamiltonian with the parameters $g_\parallel = 1.92 \pm .03$ and $g_\perp = 1.74 \pm .02$. A 15 cm length of 1% Al_2O_3:Cr showed no absorption lines for any value of magnetic field, indicating that the transitions between the Cr^{3+} ion pair levels known to exist in this energy region are strongly forbidden.

Samples of ruby reported to show far-infrared absorption lines were tested, and it was found that the splitting of the observed lines in a magnetic field was consistent with the assumption that they were due to Ti^{3+} as an unintentional impurity.

I. INTRODUCTION

In recent measurements of the far-infrared transmission of Al_2O_3 intentionally doped with Ti and V, Nelson et al.[1] and Wong et al.[2] observed absorption lines which they attributed to transitions between the electronic levels of Ti^{3+} and V^{4+} in the Al_2O_3 lattice. This assignment was reinforced by recent calculations made by Macfarlane et al.[3] of the expected energy levels of a single d electron in the Al_2O_3 crystalline field modified by a dynamic Jahn-Teller effect. The lines attributed to Ti^{3+} have a long history. Very similar lines were observed by Hadni[4] in a ruby sample with no suspected Ti impurity. The lines were then seen in Ti-doped Al_2O_3 by Perry.[5] More recently, Moser et al. observed the same lines in samples of Al_2O_3 doped with Ti, Cr, and V. Since the line strengths did not seem to correlate with analyses for Ti impurity they were attributed to lattice vibrational modes.[6] In order to resolve this discrepancy and to provide a critical test of the theory of single d electrons in Al_2O_3 we have investigated the magnetic field dependence of the far-infrared spectra of various samples of doped Al_2O_3. These included Ti, V, and Cr-doped material studied by Nelson[1] and Wong[2] and Ti and Cr-doped material related to that used by Moser et al.[6] As will be discussed below, our results confirm the assignments to electronic transitions of Ti^{3+} and V^{4+} and are in fairly good agreement with the theory.

We also investigated an absorption line near 8 cm^{-1} in the sample of Al_2O_3:V which turned out to be due to a low-lying electronic level of the $(d)^2$ system of V^{3+}. Our magnetic field results confirmed this assignment and could be fit well to the theoretical magnetic field dependence obtained from a spin-Hamiltonian.

II. EXPERIMENTAL APPARATUS

The far-infrared data in this study were obtained using the techniques of Fourier transform spectroscopy. In this method (which has been described fully elsewhere[7,8]), the spectrum is obtained by computing the Fourier transform of the interference pattern or interferogram measured using a two-beam interferometer. In practice, the interferogram is sampled at uniform intervals of Δ, the path difference between the two beams, the Fourier integral is approximated by a sum, and the spectrum is computed on a high-speed digital computer. The resolution is limited only by the finite travel of the micrometer screw driving the moveable mirror; for our apparatus this is about 5 cm, corresponding to a maximum resolution of 0.10 cm^{-1}.

Figure 1 shows the far-infrared Michelson interferometer which we constructed for use in the frequency region 2-300 cm^{-1}. It is similar to the interferometer described by Richards,[8] except that the moveable mirror is advanced by a stepping motor which is programmed to turn through a given angle of rotation each cycle. Three sets of filters can be used to remove unwanted radiation: black polyethylene at the output of the interferometer removes visible and near-infrared light; polyethylene transmission gratings of the type described by Möller and McKnight[9] can be inserted as indicated in Fig. 1; a filter wheel of various Yoshinaga filters[10] is located at the output of the instrument. The output is chopped so that lock-in detection can be used and is conveyed to the sample through a 1.1 cm i.d. light pipe.

Figure 2 shows the cryostat, which contains the sample, superconducting magnet, and detector. The sample is mounted in a light pipe which can be removed from the cryostat, and samples can be changed without appreciable loss of He. The NbZr superconducting solenoid is capable of producing a field of 55 kOe. The chamber containing the In-doped Ge bolometer detector is separated from the sample cavity by a sapphire window and has its own liquid He tank which can be pumped to provide the necessary low temperature for efficient bolometer operation. The signal from the bolometer is fed to a lock-in amplifier where it is converted to a dc voltage; the voltage is measured by a digital voltmeter and recorded on punched cards.

III. EXPERIMENTS WITH $Al_2O_3:Ti^{3+}$ AND $Al_2O_3:V^{4+}$

In the samples studied, the impurity ion is assumed to be substituted directly for an Al^{3+} ion. The Al^{3+} lattice symmetry is trigonal, but the six O^{2-} ions adjacent to an Al site lie at the corners of a not too badly distorted octahedron; thus the crystalline field seen by an ion substituted for Al is largely cubic with a small trigonal distortion. For the case of the d^1 ions Ti^{3+} and V^{4+}, this crystalline field splits the tenfold degenerate free ion energy level of the d electron into an upper level having E_g symmetry and lower A_{1g} and E_g levels. In addition, the lower E_g level is split by spin-orbit coupling and the upper E_g level is split by the Jahn-Teller effect.[11] The resulting configuration is shown in Fig. 3. Only the three lowest levels, labeled $E_{3/2}$, ${}_1E_{1/2}$, and ${}_2E_{1/2}$ in order of increasing energy, are of interest in our experiment.

The majority of our measurements were made on crystals of intentionally doped $Al_2O_3:Ti^{3+}$ and $Al_2O_3:V^{4+}$ which were immersed in liquid He to keep their temperature near $4.2^{\circ}K$. The Ti-doped samples were about 1 cm in diameter and 1 to 5 mm thick; some of them had the optic axis (referred to here as the $\underset{\sim}{c}$ axis) in the plane of the crystal (and thus perpendicular to the magnetic field), while others had the $\underset{\sim}{c}$ axis normal to the plane. By doing experiments on both types we were able to orient our solenoidal magnetic field both parallel to and perpendicular to the $\underset{\sim}{c}$ axis. The concentration of Ti was 0.15% by weight of the oxide; it is not known how much of this was in the 3+ oxidation state. The $Al_2O_3:V^{4+}$ crystal was approximately a cube 1 cm on a side; experiments were done with the $\underset{\sim}{c}$ axis parallel to and perpendicular to the magnetic field. The concentratio

of vanadium was not known. Furthermore, since the V_2O_3 structure (corresponding to V^{3+}) is the most stable state in the corundum lattice, only a small fraction of the V present was expected to be in the 4+ state.

These samples were obtained from J. Y. Wong and A. L. Schawlow and are similar to those used in their zero field measurements.[1,2] Our zero field measurements were consistent with their reported results. In the $Al_2O_3:Ti^{3+}$ sample absorption lines were seen at 37.8 cm^{-1} and 107 cm^{-1}. For the $Al_2O_3:V^{4+}$ sample a similar pair of lines was observed at 28.1 cm^{-1} and 53 cm^{-1}. For both samples the high frequency line was sufficiently broader than the low frequency line so that observation of its Zeeman splitting would have been difficult in the available magnetic field. We therefore concentrated on the low frequency lines at 37.8 cm^{-1} in $Al_2O_3:Ti^{3+}$ and 28.1 cm^{-1} in $Al_2O_3:V^{4+}$.

When a magnetic field was applied to the Ti-doped samples with $\underset{\sim}{c} \parallel \underset{\sim}{H}$, the 37.8 cm^{-1} line split into four lines as indicated in Fig. 4. The effect of the thermal depopulation of the upper Zeeman level of the ground state at 4.2°K on the relative strengths of the Zeeman components was clearly seen. If we consider the ground ($E_{3/2}$) and first excited ($_1E_{1/2}$) states to have g-values of g_0 and g_1, respectively, then the transitions between them will have effective g-values of $g_a = \frac{1}{2}(g_0 + g_1)$ and $g_b = \frac{1}{2}(g_0 - g_1)$. Applying this reasoning to our results, we obtained parallel field g-values of $g_{0\parallel} = 1.11 \pm .03$ and $g_{1\parallel} = 2.00 \pm .06$. For the samples with $\underset{\sim}{c} \perp \underset{\sim}{H}$, no broadening or splitting of the 37.8 cm^{-1} line was observed, implying that the perpendicular field g-values for both the ground and first excited states are less than 0.1.

Our results for g_0 in both the Ti and V-doped samples are in good agreement with previous results obtained by electron paramagnetic resonance. Two groups[12,13] have measured values of $g_{0\parallel} = 1.07$ and $g_{0\perp} < 0.1$ for $Al_2O_3:Ti^{3+}$. Merritt[14] has recently measured a value of $g_{0\parallel} = 1.39$ in $Al_2O_3:V^{4+}$.

IV. THEORY OF d^1 ELECTRONIC STATES

Recently, Macfarlane, Wong, and Sturge[3] considered the influence of a dynamic Jahn-Teller effect on the energy levels of a d^1 electronic system in the Al_2O_3 crystal symmetry. They found that the first order effect uniformly reduced the matrix elements of the trigonal and spin-orbit crystalline field operators, whereas the inclusion of second order effects introduced non-linear corrections to the static crystalline field results and allowed reasonable agreement with experimental data.

As shown in Fig. 3, the effect of the trigonal and spin-orbit operators on the $^2T_2$ octahedral level is a splitting of this sixfold degenerate level into three Kramers doublets $E_{3/2}$, $_1E_{1/2}$, and $_2E_{1/2}$. Using representative values for the trigonal and spin-orbit coupling parameters for $Al_2O_3:Ti^{3+}$, Macfarlane et al. calculated the values $\delta_1 = 109\ cm^{-1}$ and $\delta_2 = 771\ cm^{-1}$, which are much larger than the experimental values of $37.8\ cm^{-1}$ and $107\ cm^{-1}$, respectively. Clearly, static crystal field theory alone cannot account for the experimental observations.

The Jahn-Teller effect results from the coupling of an electronic system in a non-Kramers degenerate state to a nuclear displacement which lifts the degeneracy. The result is a displacement of the electronic system to a new position of minimum potential energy. The gain in potential energy E_{JT} is balanced by the loss in elastic energy due to the displacement from the equilibrium position. For the octahedral $^2T_2$ level in Al_2O_3 there are three equivalent configurations to which the system can distort, and in the static Jahn-Teller effect, the

electronic system randomly occupies one of these three energy minima, provided $k_B T << E_{JT}$. When a perturbation to the octahedral field (such as a trigonal field or spin-orbit coupling) causes energy changes in the $^2T_2$ level which are comparable with the Jahn-Teller energy E_{JT}, no such static distortion occurs, but the complex exhibits a coupled motion of the electrons and the lattice vibrational modes. This situation is referred to as the dynamic Jahn-Teller effect, and in the present case it causes a partial averaging of the trigonal and spin-orbit perturbations. To first order all matrix elements of these operators are reduced by a quenching factor γ (Ham effect[15]). This first order ocrrection is insufficient to explain the experimental data, since the Ham effect would reduce the values of δ_1 and δ_2 by the same multiplicative factor, whereas the experimental values are respectively 0.35 and 0.14 of the estimated static crystalline field values.

Macfarlane et al. then considered second order perturbation effects within the manifold of basis states for the $^2T_2$ level and between the basis states for $^2T_2$ and those for ^2E. They obtained analytical expressions for the energy splittings δ_1 and δ_2 as well as the g-values for the Zeeman splitting of the $E_{3/2}$, $_1E_{1/2}$, and $_2E_{1/2}$ levels. The independent variables involved are the trigonal and spin-orbit coupling parameters v and ζ, and the quenching factor $\gamma = \exp(-3E_{JT}/2\hbar\omega)$, where E_{JT} is the Jahn-Teller energy and $\hbar\omega$ is the energy of the vibronic mode which is responsible for the Jahn-Teller effect.

The analytical expressions of Macfarlane et al. were fitted to our experimental data. Several results of the trial-and-error procedure used are tabulated in Table I, along with the data. The analytical

expressions are quite complicated and are sufficiently sensitive to a small change in some of the variables to make the fit somewhat arbitrary. Two sets of theoretical parameters chosen primarily to fit the zero field data for δ_1 and δ_2 are given in Table I to display this sensitivity.

V. RUBY EXPERIMENTS

In 1964 Hadni observed absorption lines in ruby at 37 cm^{-1} and 100 cm^{-1} which he assigned to exchange coupling between pairs of Cr^{3+} ions.[4] These pair lines have been observed optically, but the direct transition is between states of different spin and is forbidden. Nelson et al.[1] measured the far-infrared transmission of a sample of 1% Cr_2O_3 in Al_2O_3 which was 15 cm in length and observed no absorption lines. We repeated his experiment with the same sample and obtained similar negative results for all values of applied magnetic field. These results, as well as the similarity in frequency, width, and relative strength between the lines seen by Hadni and those subsequently found for Ti^{3+} suggest strongly that he was seeing Ti^{3+} as an unintentional impurity in his ruby.

Later, Moser et al. reported[6] lines at 37.75 cm^{-1} and 108 cm^{-1} in samples of Al_2O_3 doped with Ti, V, and Cr. These were attributed to lattice vibrational modes because the line strengths did not seem to correspond to those expected from analyses of the amount of Ti impurity present. However, the coincidence of their reported lines with the Al_2O_3:Ti^{3+} spectrum and the lack of any lines in our sample of Al_2O_3:Cr^{3+} raised doubts as to the correctness of this assignment. We performed transmission measurements on four of their samples and found that the 37.8 cm^{-1} and 107 cm^{-1} lines were not always observed, but when they were, the 37.8 cm^{-1} line split in a magnetic field in a manner consistent with the assumption that it was due to Ti^{3+}. A one cm thick 1.2% ruby of Swiss origin was also found to have absorptions characteristic of Ti^{3+}.

VI. $Al_2O_3:V^{3+}$ EXPERIMENTS

The V^{3+} ion has two d electrons, and the effect of the Al_2O_3 crystalline field on the free ion ^3F state, shown in Fig. 6, is more complicated than for V^{4+}. Only the lowest level ($^3A_2$) is of interest here, since the trigonal splitting is believed[16] to be ~1200 cm^{-1}, so the mixing between the $^3A_2$ and ^3E states is small.

The sample was the same one used for the $Al_2O_3:V^{4+}$ experiments, and all measurements were done with the sample at 4.2°K. For no applied field, a strong line was observed at 8.25 cm^{-1}. In a field parallel to the c axis, this line split linearly with field. When the field was applied perpendicular to the c axis, a quadratic Zeeman effect was observed. Figure 7 shows the behavior of the 8.25 cm^{-1} line in both field orientations.

If we consider the ground ($^3A_2$) state only, the magnetic properties can be described by means of the spin-Hamiltonian:

$$\mathcal{H} = DS_z'^2 + g_{\parallel}\beta S_z'H_z + g_{\perp}\beta(S_x'H_x + S_y'H_y)$$

where $\underset{\sim}{S}'$ is the effective spin of the ground state ($|S'| = 1$). Because of the large trigonal splitting and the small spin-orbit splitting very little mixing between the spin states of $^3A_2$ and those of higher levels is expected, so the spin states $|+\rangle$, $|o\rangle$, $|-\rangle$ are reasonably good basis states for $^3A_2$. Any mixing will tend to quench the Zeeman splitting of the $^3A_2$ level, however, giving values of $g_{\parallel}$ and $g_{\perp}$ smaller than 2.0 by an amount which depends on the ratio of the spin-orbit coupling to the trigonal splitting.[16]

The first term in $\mathcal{H}$ splits the $^3A_2$ level into two levels separated by D, the doubly degenerate M = ±1 level lying higher. The effect of a magnetic field parallel to $\underset{\sim}{c}$ is represented by the second term; this perturbation does not mix states of different M and the M = ±1 level is split by $2g_{\parallel}\beta H$, as shown in Fig. 6. The third term in $\mathcal{H}$ represents a magnetic field perpendicular to $\underset{\sim}{c}$, which mixes the three spin states. The resulting transitions start out at D and both curve upward as the field increases. Figure 7 shows the experimental data (points) and the theoretical results (lines) obtained by adjusting $g_{\parallel}$ and $g_{\perp}$ for the best fit. An excellent fit is obtained for both field orientations which yields the results $g_{\parallel} = 1.92 \pm .03$ and $g_{\perp} = 1.74 \pm .02$.

Our direct measurements of the transitions determines all three parameters in the spin-Hamiltonian to a high degree of precision. A value of D = 8 cm^{-1} was obtained by Pryce and Runciman[17] from the difference between two optical absorption lines at about 21,000 cm^{-1}; their Zeeman experiments indicated $g_{\parallel} \lesssim 2$. Zverev and Prokhorov[18] investigated the electron paramagnetic resonance between the M = ±1 levels and obtained $g_{\parallel} = 1.92 \pm .01$, in excellent agreement with our result. The only known measurement of $g_{\perp}$ was made by van den Handel and Siegert,[19] who obtained the value $g_{\perp} = 1.82$ from susceptibility measurements of vanadium-ammonium alum.

VII. CONCLUSIONS

From our experiments on $Al_2O_3:Ti^{3+}$ and $Al_2O_3:V^{4+}$ we conclude that the observed absorption lines are due to low-lying electronic states of the nominal impurity ion in the effective crystalline field of the host lattice. The Zeeman splitting of the low frequency absorption line in each case shows that they cannot be due to lattice vibrational modes. The general agreement of our results with the theory of Macfarlane et al. leads to the conclusion that the vibronic interaction correction to the static crystalline field can largely explain the electronic levels of a d^1 impurity ion in Al_2O_3. As shown in Table I, the agreement between theory and experiment is not perfect. Since our fit was made by adjustment of the parameters to fit only two of the five variables (δ_1 and δ_2), there is considerable freedom of choice for the values of several parameters. We found that the value of $g_{0\|}$ was rather insensitive to changes in the trigonal and spin-orbit parameters, and the 10% disagreement between experimental and theoretical values of $g_{0\|}$ for $Al_2O_3:V^{3+}$ indicates that improvement of the theory is desirable.

Our experiments on $Al_2O_3:V^{3+}$ are in agreement with previous work and yield more precise values of the spin-Hamiltonian parameters.

ACKNOWLEDGMENTS

We are grateful to Professor A. L. Schawlow and Dr. J. Y. Wong for providing the samples of Al_2O_3:Ti, Al_2O_3:V, and Al_2O_3:Cr used in our experiments, and to Dr. R. M. Macfarlane and Dr. J. Y. Wong for helpful discussions and for making their calculations available to us prior to publication. Thanks are also due Dr. J. F. Moser and Dr. F. K. Kneubühl for allowing us to measure their samples and Dr. G. A. Slack for suggesting the investigation of the V^{3+} line.

This work was performed under the auspices of the United States Atomic Energy Commission.

Table I.

Sample	v	ζ	E_{JT}	δ_1	δ_2	$g_{0\parallel}$	$g_{0\perp}$	$g_{1\parallel}$	$g_{1\perp}$	$g_{2\parallel}$
$Al_2O_3:Ti^{3+}$	700	120	200	44.98	104.21	1.16	0.0	-2.22	< 0.2	1.88
	680	90	187	37.96	106.53	1.13	0.0	-2.30	< 0.2	1.93
	Experimental			37.8	107	1.11	< 0.1	-2.00	< 0.1	
$Al_2O_3:V^{4+}$	970	195	320	27.93	53.15	1.59	0.0	-2.00	< 0.5	1.86
	750	290	333	27.80	53.20	1.60	0.0	-1.70	< 0.5	1.66
	Experimental			28.1	53	1.43	< 0.2	-1.43	< 0.2	
$Al_2O_3:V^{3+}$	Experimental			$D = 8.25\ cm^{-1}$						
				$g_{\parallel} = 1.92 \pm .03$						
				$g_{\perp} = 1.74 \pm .02$						

REFERENCES

1. E. D. Nelson, J. Y. Wong, and A. L. Schawlow, Phys. Rev. 156, 298 (1967).

2. J. Y. Wong, M. J. Berggren, and A. L. Schawlow, J. Chem. Phys. (to be published).

3. R. M. Macfarlane, J. Y. Wong, and M. D. Sturge, Phys. Rev. 166, 250 (1968).

4. A. Hadni, Phys. Rev. 136, A758 (1964).

5. C. H. Perry, R. Geick, and E. F. Young, Appl. Optics 5, 1171 (1966).

6. J. -F. Moser, W. Zingg, H. Steffen, and F. K. Kneubühl, Phys. Letters 24A, 411 (1967).

7. J. Connes, Rev. Opt. 40, 45, 116, 171, and 231 (1961).

8. P. L. Richards, in Spectroscopic Techniques for Far Infra-red, Submillimetre, and Millimetre Waves, D. H. Martin, editor (North-Holland Pub. Co., Amsterdam, 1967), Chap. 7; J. Opt. Soc. Am. 54, 1474 (1964).

9. K. D. Möller and R. V. McKnight, J. Opt. Soc. Am. 55, 1075 (1965).

10. Y. Yamada, A. Mitsuishi, and H. Yoshinaga, J. Opt. Soc. Am. 52, 17 (1962).

11. D. S. McClure, J. Chem. Phys. 36, 2757 (1962).

12. N. E. Kask, L. S. Kornienko, T. S. Mandel'shtam, and A. M. Prokhorov, Fiz. Tverd. Tela 5, 2306 (1963); [translation: Sov. Phys.--Solid State 5, 1677 (1964)].

13. D. W. Feldman, D. C. Burnham, and J. G. Castle, Jr., Westinghouse Research Lab., Quarterly Scientific Report No. 4, 1964 (unpublished), Contract No. AF 19(628)1640, AFCRL64-665.

14. F. R. Merritt (private communication).

15. F. S. Ham, Phys. Rev. 138, A1727 (1965).

16. A. Abragam and M. H. L. Pryce, Proc. Roy. Soc. (London) A205, 135 (1951).

17. M. H. L. Pryce and W. A. Runciman, Discussions Faraday Soc. 26, 34 (1958).

18. G. M. Zverev and A. M. Prokhorov, Soviet Phys. JETP 7, 707 (1958).

19. J. van den Handel and A. Siegert, Physica 4, 871 (1937).

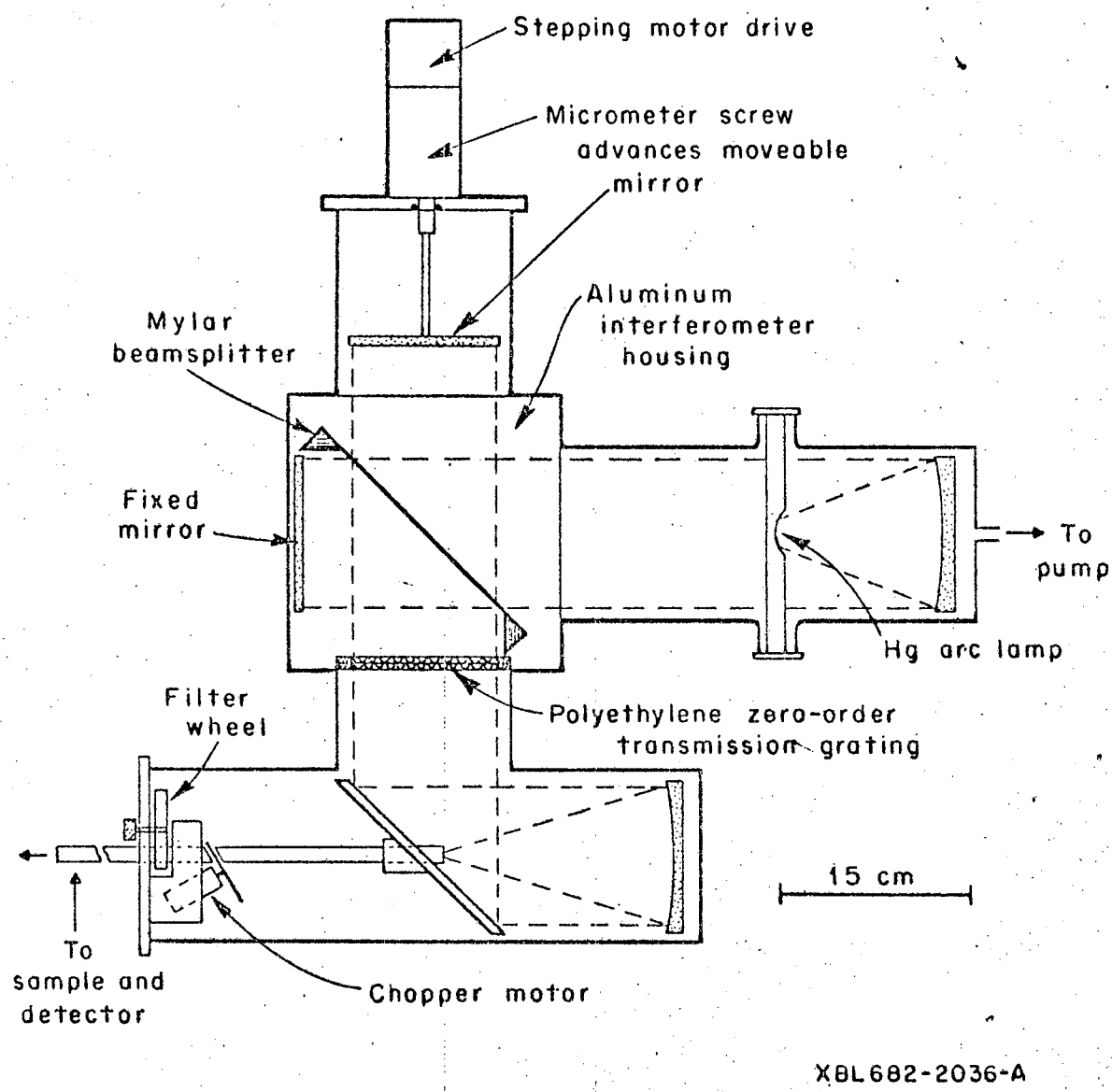
Stepping motor drive
Micrometer screw advances moveable mirror
Aluminum interferometer housing
Mylar beamsplitter
Fixed mirror
To pump
Hg arc lamp
Filter wheel
Polyethylene zero-order transmission grating
15 cm
To sample and detector
Chopper motor
XBL682-2036-A

Fig. 1

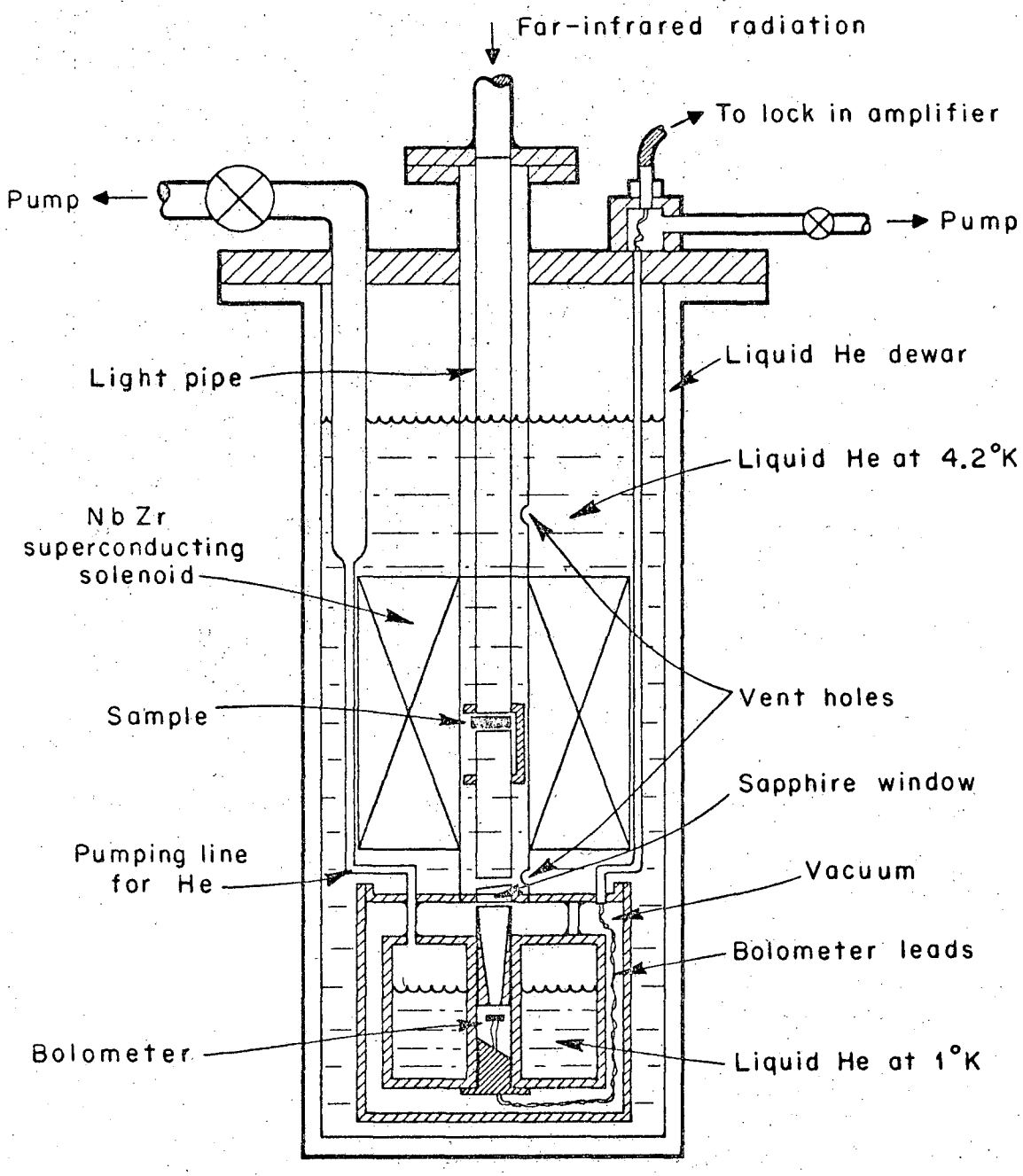

XBL682-2034-A

Fig. 2

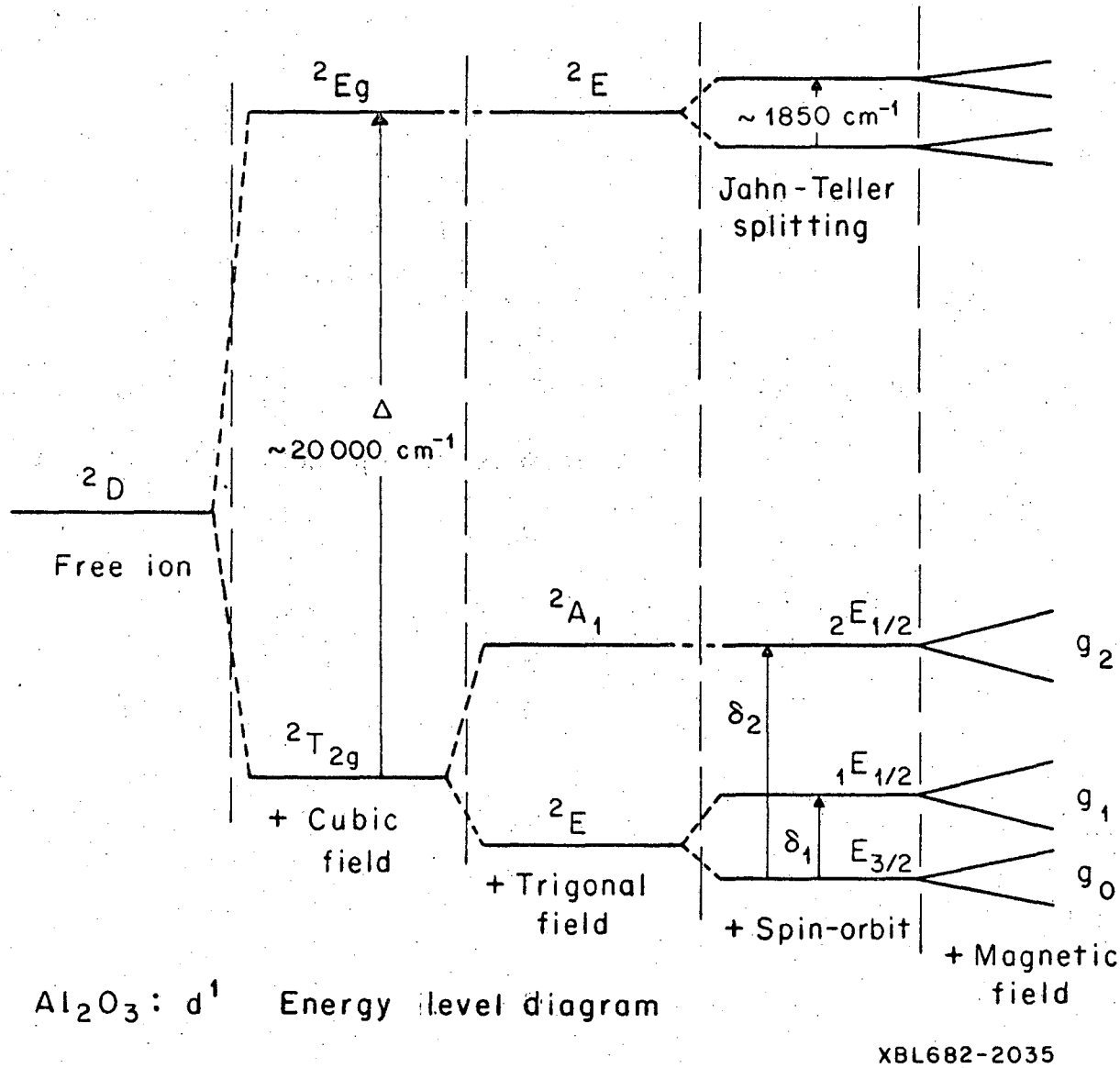
^2E_g
^2E
~ 1850 cm^{-1}
Jahn-Teller splitting
Δ
~20 000 cm^{-1}
^2D
Free ion
$^2A_1$
$^2E_{1/2}$
g_2
δ_2
$^2T_{2g}$
$^1E_{1/2}$
g_1
+ Cubic field
^2E
δ_1
$E_{3/2}$
g_0
+ Trigonal field
+ Spin-orbit
+ Magnetic field
Al_2O_3 : d^1 Energy level diagram
XBL682-2035

Fig. 3

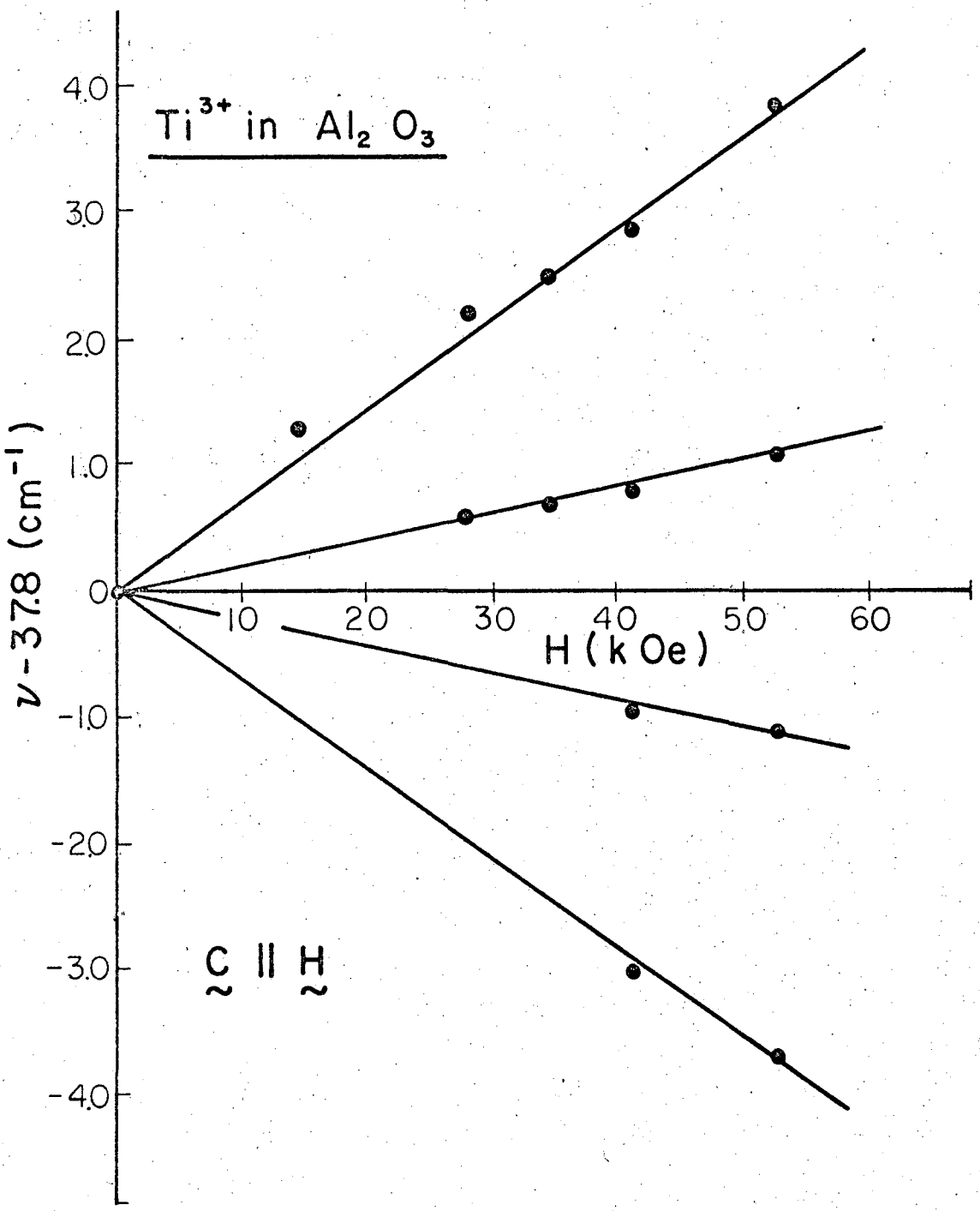

XBL681-1528-A

Fig. 4

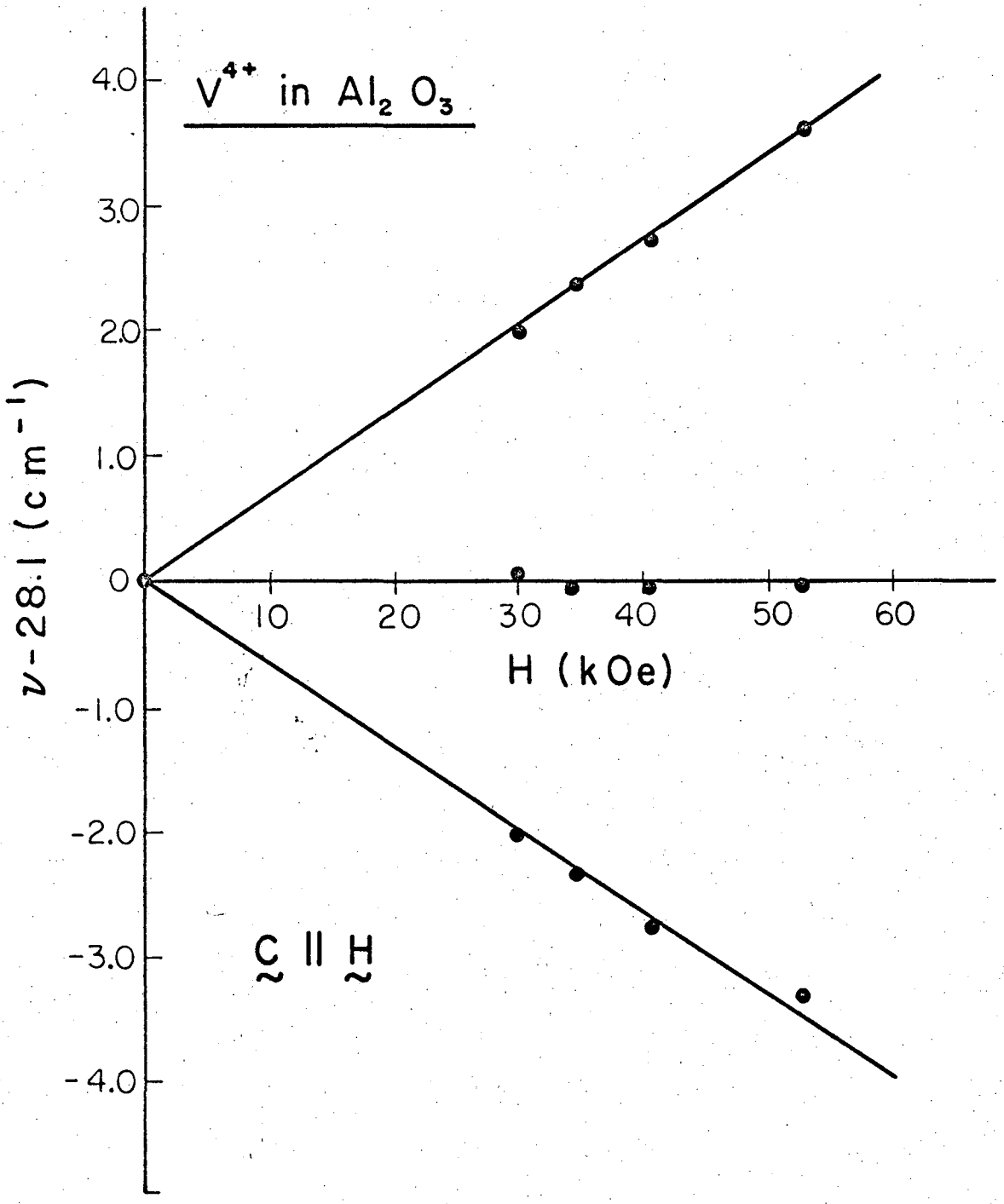

XBL681-1529-A

Fig. 5

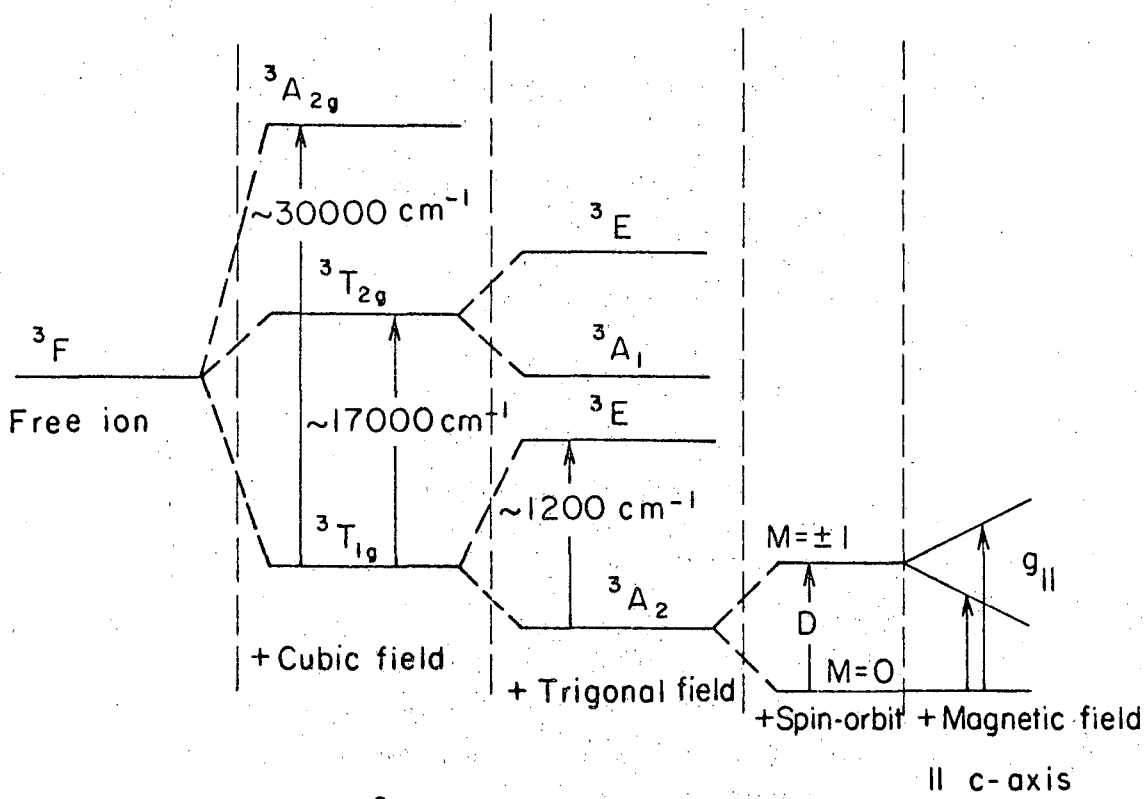

Al_2O_3: d^2 Energy level diagram

XBL684-2514

Fig. 6

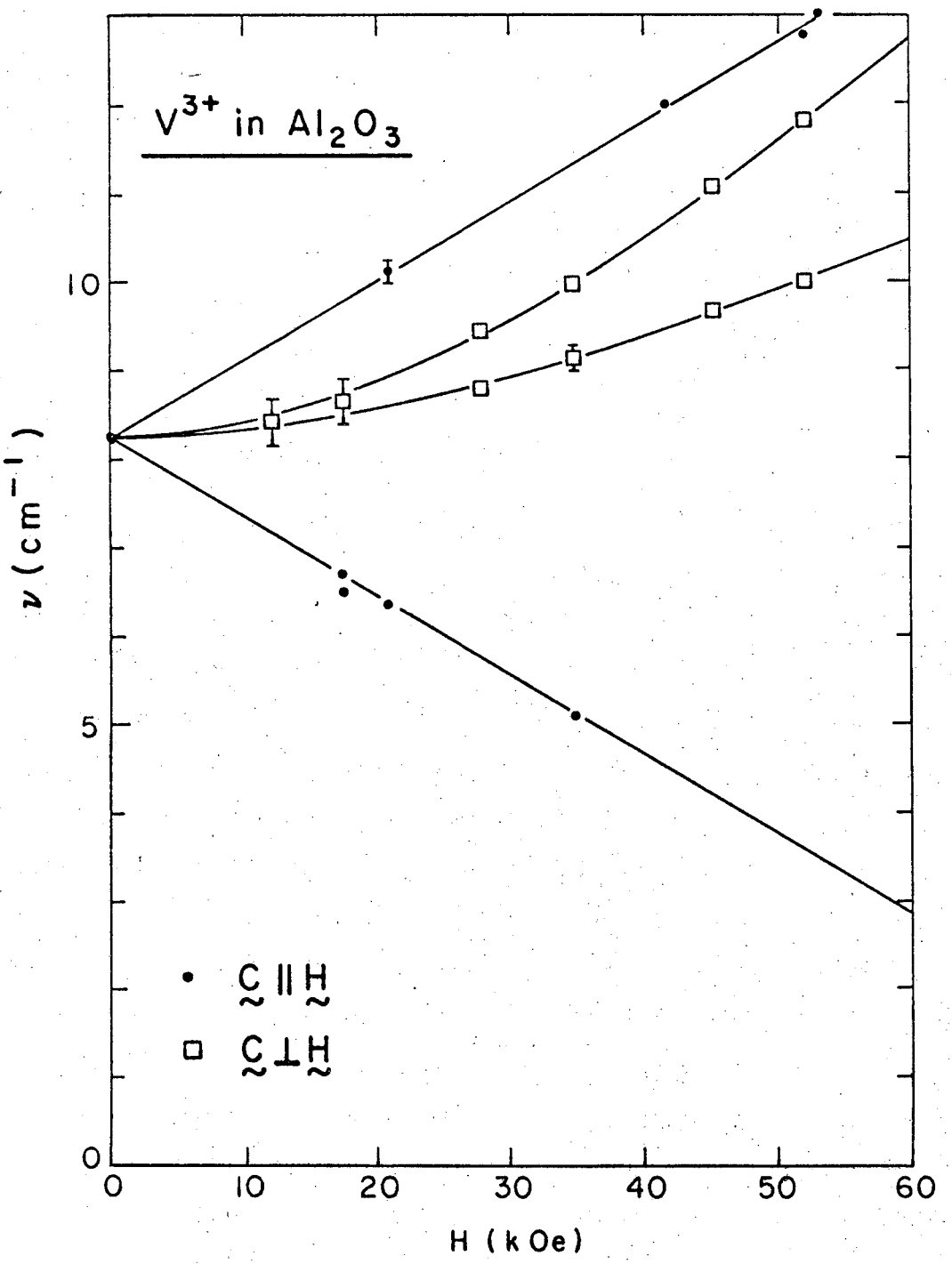

XBL 684-2515-A

Fig. 7

This report was prepared as an account of Government sponsored work. Neither the United States, nor the Commission, nor any person acting on behalf of the Commission:

A. Makes any warranty or representation, expressed or implied, with respect to the accuracy, completeness, or usefulness of the information contained in this report, or that the use of any information, apparatus, method, or process disclosed in this report may not infringe privately owned rights; or

B. Assumes any liabilities with respect to the use of, or for damages resulting from the use of any information, apparatus, method, or process disclosed in this report.

As used in the above, "person acting on behalf of the Commission" includes any employee or contractor of the Commission, or employee of such contractor, to the extent that such employee or contractor of the Commission, or employee of such contractor prepares, disseminates, or provides access to, any information pursuant to his employment or contract with the Commission, or his employment with such contractor.